Heavy-light mesons and baryons with *b* quarks

A. Ali Khan,[1] T. Bhattacharya,[2] S. Collins,[3] C. T. H. Davies,[3] R. Gupta,[2] C. Morningstar,[4] J. Shigemitsu,[5] and J. Sloan[6,*]

[1]*Center for Computational Physics, University of Tsukuba, Tsukuba, Ibaraki 305-8577, Japan*
[2]*Los Alamos National Laboratory, Los Alamos, New Mexico 87545*
[3]*Department of Physics & Astronomy, University of Glasgow, Glasgow, G12 8QQ United Kingdom*
[4]*Physics Department, Florida International University, Miami, Florida 33199*
[5]*Physics Department, The Ohio State University, Columbus, Ohio 43210*
[6]*Physics Department, University of Kentucky, Lexington, Kentucky 40506*
(Received 6 January 2000; published 27 July 2000)

We present lattice results for the spectrum of mesons containing one heavy quark and of baryons containing one or two heavy quarks. The calculation is done in the quenched approximation using the NRQCD formalism for the heavy quark. We analyze the dependence of the mass splittings on both the heavy and the light quark masses. Meson *P*-state fine structure and baryon hyperfine splittings are resolved for the first time. We fix the *b* quark mass using both M_B and M_{Λ_b}, and our best estimate is $m_b^{\overline{MS}}(m_b^{\overline{MS}}) = 4.35(10)(^{-3}_{+2})(20)$ GeV. The spectrum, obtained by interpolation to m_b, is compared with the experimental data.

PACS number(s): 12.38.Gc, 14.20.Mr, 14.40.Nd, 14.65.Fy

I. INTRODUCTION

The spectrum and decays of hadrons containing *b* quarks will be measured in precision experiments at the *B* factories. It is therefore important to calculate the spectrum expected from QCD, both as a test of the theory and to predict the masses of states not yet observed. This paper reports on results of a lattice calculation of the heavy-light spectrum using the non-relativistic formulation of QCD (NRQCD) for heavy quarks [1], and the tadpole-improved clover action for light quarks. This approach allows us to have better control over discretization errors in both the heavy and the light quark sectors.

Lattice QCD allows us to investigate the dependence of the meson and baryon mass splittings on the heavy and light quark masses. For this purpose we simulate three values of light quark masses in the range $0.8m_s$–$1.3m_s$, and six values of heavy quark masses in the range 3–20 GeV. The NRQCD formalism is ideally suited to study such a wide range of heavy quark masses at $1/a = 1.92$ GeV, the lattice spacing we use. For the light quarks we use the tadpole-improved clover action which has discretization errors of $O(\alpha_s a)$ and these are expected to be small at this lattice spacing. These improvements make it possible to perform reliable comparisons with both the experimental *b* spectrum and expectations based on heavy quark symmetry.

The phenomenological interest in the decay rates of hadrons containing *b* quarks stems from the important role they play in the determination of the Cabibbo-Kobayashi-Maskawa matrix elements. Two quantities that are used as input in the analyses of experimental data are $m_b^{\overline{MS}}(m_b^{\overline{MS}})$ and the decay constants f_B and f_{B_s}. Here we shall present results for the *b* quark mass, while the calculation of decay constants has already been reported in a companion paper [2].

This paper is organized as follows. In Sec. II we briefly review the experimental situation and provide a justification for the NRQCD approach to heavy quarks. The parameters used in the simulations are given in Sec. III. Section IV describes the determination of the *b* quark mass. Our results on the heavy-light meson spectrum are presented in Sec. V along with a discussion of the spin-independent and spin-dependent mass splittings. Baryons containing one heavy and two light quarks are discussed in Sec. VI. In Sec. VII we give a brief description of our results on baryons containing two (degenerate) heavy quarks and one light quark. This is followed by a determination of HQET parameters in Sec. VIII. Finally, we summarize our main conclusions in Sec. IX.

II. PHENOMENOLOGICAL BACKGROUND

The NRQCD approach for simulating *b* quarks is justified because the typical velocity of the heavy quark is small, $v/c \sim O(\Lambda_{\text{QCD}}/M) \sim 0.05$–0.1. This is corroborated by the experimental observation that all splittings are much smaller than the masses, and the hadron masses are dominated by the heavy quark mass. Thus a very natural picture of the heavy-light system is a ''hydrogen atom'' composed of the light degrees of freedom bound in the background of an almost static color source. Within this model one can distinguish between spin-independent splittings in the spectrum dominated by radial and/or orbital excitations of the light quark, and spin-dependent ones dominated by the spin-flip energy of the heavy quark. These two types of splittings have distinct behavior as a function of the heavy quark mass. Spin-independent splittings survive the infinite heavy quark mass limit whereas the spin-dependent ones do not.

The experimental data plotted in Fig. 1 show that the spin-independent splittings are often insensitive to the mass of the heavy quark. In fact one finds in many cases that the insensitivity persists down to the strange quark mass. Spin-dependent splittings, on the other hand, are found to increase

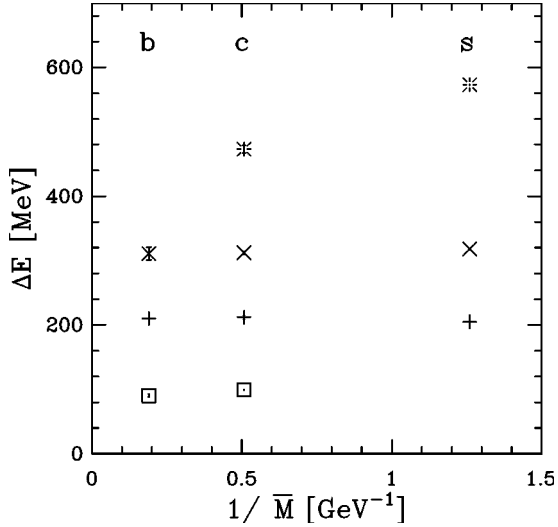*Present address: Spatial Technologies, Boulder, CO.

FIG. 1. Experimental spin-independent mass splittings for hadrons with one heavy quark ($h = b$, c, or s) as a function of the spin-averaged meson mass $\bar{M} \equiv (M_H + 3M_{H*})/4$ where H denotes a generic heavy meson. Squares denote the B_s-B_d and the D_s-D_d splitting. Pluses stand for the spin-averaged Σ-Λ splitting (we have used the DELPHI measurement of Σ_b [3]). The splitting between the Λ and the spin-averaged S state meson is denoted by crosses. Bursts denote the spin-averaged P-S splitting.

with the inverse heavy quark mass as shown in Fig. 2. An analysis with a phenomenologically determined potential is in agreement with these results, however there is considerable uncertainty in how to model the light degrees of freedom (see [5] and references therein). Simulations of lattice
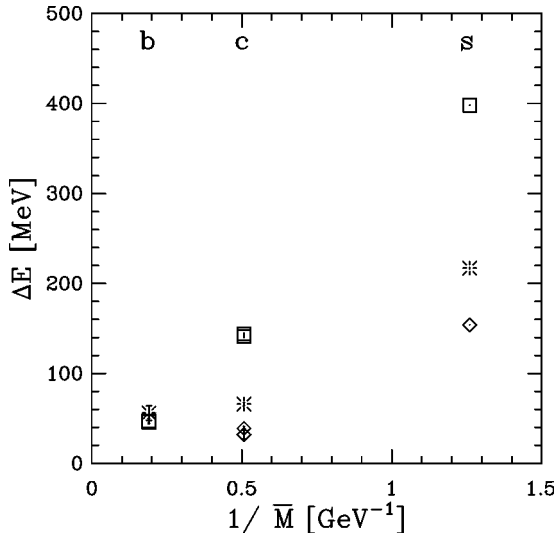

FIG. 2. Experimental spin-dependent mass splittings for hadrons with one heavy quark. $\bar{M}$ is defined in Fig. 1. Squares denote the S state hyperfine splitting for B, B_s, D, D_s, and K mesons. Diamonds denote the splitting between P states with $j_l = 3/2$. These are known only for D, D_s, and K mesons. The Σ^*-Σ splitting for baryons is denoted by bursts. (For a discussion of the possibility that some of the Σ_c and Σ_b baryons have been misidentified experimentally see Ref. [4].)

TABLE I. A summary of the heavy and light quark mass parameters, aM^0 and κ, used in the simulation and the resulting mass of pions composed of degenerate light quarks. We also list the values of the stability parameter n used in the heavy quark evolution [2].

Heavy quark parameters					
aM^0	1.6	2.0	2.7	4.0	7.0	10.0
n	2	2	2	1	1	1
Light quark parameters		
κ	0.1369	0.1375	0.13808
am_π	0.423(7)	0.362(11)	0.298(4)

QCD using a non-relativistic formulation for heavy quarks provide estimates without resort to modeling.

The NRQCD formulation has been discussed in [1,6]. It has been very successful in the study of heavy quarkonia [6], and we apply it to predict the heavy-light spectrum here. Results using alternate formulations, static heavy quarks or standard (Wilson or clover) discretization of the Dirac operator mostly extrapolated from the charm region, can be found in [7–11] and we shall compare against them at appropriate places.

III. SIMULATION PARAMETERS

The statistical sample consists of the same 102 quenched configurations, at $\beta = 6.0$ with lattice size $16^3 \times 48$, as used in our study of decay constants [2]. The NRQCD action, the evolution equation for calculating the heavy quark propagator, the method used for setting the lattice scale, and the fixing of light and strange quark masses are also the same. The list of quark masses used in our simulation are reproduced in Table I, and the operators used to study the various states, are given in Table II.

We estimate that the significant sources of systematic errors in this calculation are finite volume, finite lattice spacing, quenching, uncertainties in determining a, fixing the strange quark mass and perturbative corrections. For a lattice size of ≈ 1.6 fm, finite volume effects are not expected to be significant for the lower lying S state mesons. However, there are indications that the wave functions for P states and the baryons are more extended [8] and finite size effects in these states should therefore be larger. We cannot comment on this as we have results on only one lattice volume. The $O(\alpha_s a)$ error associated with the tadpole improved clover light fermions is expected to be a few percent at this β [12]. A detailed study of the scaling behavior of the heavy-light spectrum is discussed in Ref. [13]. Quenching errors remain unknown. However, since the B spectrum is dominated by the light quark degrees of freedom, we expect that using light spectroscopic quantities to fix a compensates for part of this uncertainty.

The central value of lattice scale we use is $1/a = 1.92(7)$ GeV as obtained from M_ρ. To estimate the systematic error in this we repeat our bootstrap analyses with $1/a = 1.8$ and 2 GeV as discussed in [2]. We obtain $\kappa_l = 0.13917(9)$, corresponding to the light quark mass $m_l = 1/2(m_u + m_d)$, by linearly extrapolating M_π^2/M_ρ^2 to

TABLE II. The operators used to study the various states. h stands for the two-component heavy quark spinor, u and d for the upper two components of two flavors of light quark spinors. $\vec{\Delta}$ is the ordinary derivative in the Coulomb gauge. The symbols $h_\uparrow$ and $h_\downarrow$ stand for the $s_z = +1/2$ and $-1/2$ components of h respectively. The baryon operators for $s_z < 0$ are constructed from the corresponding $s_z > 0$ operators by interchanging $\sigma_+ \leftrightarrow \sigma_-$ and $\uparrow \leftrightarrow \downarrow$. The Ξ baryons are obtained by replacing one of the light flavors in Σ by an s, and the Ω by replacing both light quarks by ss. For the heavy-heavy-light baryons, the operators are identical except u and d are to be interpreted as two flavors of heavy quarks and h as the light or s quark. The $^3P_2$ states decompose, under the cubic group, into two representations labeled T and E. Our $j=2P$ states are spin-averaged over both lattice representations: $^3P_2 = [3\ ^3P_2(T) + 2\ ^3P_2(E)]/5$.

State		Operator
$^1S_0$		$\bar{u}h$
$^3S_1$		$\bar{u}\vec{\sigma}h$
$^1P_1$		$\bar{u}\vec{\Delta}h$
$^3P_0$		$\bar{u}\vec{\sigma}\cdot\vec{\Delta}h$
$^3P_1$		$\bar{u}\vec{\sigma}\times\vec{\Delta}h$
$^3P_2$	(T)	$\bar{u}(\sigma_i\Delta_j + \sigma_j\Delta_i)h$
$^3P_2$	(E)	$\bar{u}(\sigma_i\Delta_i - \sigma_j\Delta_j)h$
Λ	$(s_z = +1/2)$	$\bar{u}^c d\, h_\uparrow$
Σ	$(s_z = +1/2)$	$(\bar{u}^c\sigma_z d\, h_\uparrow - \sqrt{2}\bar{u}^c\sigma_+ d\, h_\downarrow)/\sqrt{3}$
Σ^*	$(s_z = +3/2)$	$\bar{u}^c\sigma_+ d\, h_\uparrow$
Σ^*	$(s_z = +1/2)$	$(\sqrt{2}\bar{u}^c\sigma_z d\, h_\uparrow + \bar{u}^c\sigma_+ d\, h_\downarrow)/\sqrt{3}$

$137^2/770^2$. We cannot resolve a curvature in the light quark mass dependence, and do not assign a systematic error in κ_l. To determine the strange quark mass, we use three different methods. By fixing the ratio M_K^2/M_π^2 to its physical value, we obtain $\kappa_s = 0.13755(13)$. Using the ratios M_{K*}/M_ρ and M_ϕ/M_ρ, gives $\kappa_s = 0.13719(25)$ and $0.13717(25)$ respectively. Since the latter two agree within errors, we only give the results using M_K and M_{K*}. For our final results, we use κ_s from M_K, and determine the systematic error using κ_s from $K*$.

In our final results, the first error we quote comes from a bootstrap analysis using $a^{-1} = 1.92(7)$ GeV, the second from the scale uncertainty, and where applicable, the third from the uncertainty in the strange quark mass. We comment on the uncertainty due to using 1-loop perturbative expressions and in fixing the b quark mass below.

A summary of some of the important features of the raw lattice data is as follows. (i) The data at $aM^0 = 7.0$ and 10.0 are not as reliable as that for $aM^0 \leq 4.0$ (there are no clear plateaux in the effective mass plots). They are, therefore, used only in the estimation of HQET parameters, where we have chosen states and operators with the best signal. (ii) The calculation of P state correlation functions has been done for only $aM^0 = 1.6, 2.0, 2.7$.

Lastly, we fix the bare b quark mass aM_b^0 as follows. In NRQCD and the static theory, E_{sim}, the rate of exponential fall-off of the heavy-light meson correlators, is not the meson mass, but is related to it by the shift,

TABLE III. The stability parameter n and the 1-loop perturbative estimates of the mass renormalization constant Z_m, the zero point shift of the heavy quark energy E_0, and the mass shift $\Delta = Z_m M^0 - E_0$ using the q^* calculated with the Hornbostel-Lepage procedure [14]. Errors associated with numerical integration of the 1-loop expressions are insignificant compared to other systematic errors.

aM^0	n	Z_m	aE_0	$a\Delta$
1.6	2	1.18	0.23	1.64
2.0	2	1.14	0.28	2.02
2.7	2	1.09	0.27	2.68
4.0	1	1.05	0.27	3.90
7.0	1	1.00	0.28	6.74
10.0	1	0.98	0.28	9.54

$$\Delta = M_{\text{hadron}} - E_{\text{sim}} = Z_m M^0 - E_0. \tag{1}$$

Here Z_m is the renormalization constant connecting the bare quark mass to the pole mass, and E_0 is the shift in the energy of the quark. As discussed in more detail in Ref. [2], we employ three different methods to calculate the meson mass: (i) M_{kin} extracted directly from the dispersion relation of the heavy-light meson; (ii) M_{pert} obtained by evaluating the mass shift Δ perturbatively; and (iii) M' using the Δ obtained from the dispersion relation of the heavy-heavy meson at the same aM^0 value. The perturbative results for Z_m, E_0 and Δ are given in Table III.[1]

In the perturbative analyses, we use $\alpha_s = \alpha_P$ defined in Ref. [15]. The relevant scale q^* at which to evaluate the running coupling α_P is chosen separately for each process using an extension [14] of the Lepage-Mackenzie scale-setting prescription [16]. The choice of scale advocated in the original Lepage-Mackenzie scheme eliminates the $O(\alpha_s^2)$ correction in the bubble summation approximation. This procedure can fail, however, when the one-loop contribution becomes small. Hornbostel and Lepage [14] have recently extended the method to overcome this difficulty by taking into account higher-order terms in the bubble summation approximation. Their extension reduces to the original Lepage-Mackenzie prescription when the one-loop term is not small due to large cancelling contributions.

The perturbative series for Z_m has an infra-red renormalon ambiguity [17], which is typically characterized by an uncertainty of $O(\Lambda_{QCD}/M)$. Since this is comparable to the entire $O(\alpha_s)$ correction, we shall use the latter as the estimate of the perturbative error in the determination of M_{pole}.

All three methods for estimating the B meson mass give compatible results for $aM^0 \leq 4$ as shown in Table IV. These estimates differ slightly from those in Ref. [2] due to a re-analysis of the data and different choice of q^*. Unfortu-

---

[1]The perturbative calculations have been done for a slightly different discretization of $F_{\mu\nu}$, i.e. a four leaf clover rather than the two leaf version used in the evolution equation. We expect the difference to be insignificant.

TABLE IV. E_{sim} and pseudoscalar meson masses in lattice units extrapolated-interpolated to κ_l and κ_s. Meson masses have been calculated from the heavy-light dispersion relation (M_{kin}), using Δ from heavy-heavy spectroscopy (M'), and from perturbation theory (M_{pert}).

	κ_l				κ_s			
aM^0	aE_{sim}	aM_{kin}	aM'	aM_{pert}	aE_{sim}	aM_{kin}	aM'	aM_{pert}
1.6	0.427(7)	2.16(13)	2.08(3)	2.07(4)	0.474(4)	2.21(9)	2.13(3)	2.11(2)
2.0	0.443(8)	2.57(18)	2.46(4)	2.46(2)	0.490(4)	2.63(13)	0.50(4)	2.51(1)
2.7	0.459(7)	3.30(30)	3.15(7)	3.14(2)	0.504(4)	3.35(21)	3.20(7)	3.18(1)
4.0	0.468(8)	4.76(65)	4.46(11)	4.37(7)	0.513(5)	4.74(43)	4.50(11)	4.41(7)
7.0	0.469(9)	8.9(24)		7.21(21)	0.516(5)	8.5(15)		7.26(21)
10.	0.471(9)	15(7)		10.01(35)	0.515(5)	13(4)		10.1(3)

nately, the most direct method, using the heavy-light dispersion relation, has large errors. The method using Δ extracted from heavy-heavy mesons is more accurate for $aM^0 \lesssim 4.0$. For $aM^0 = 7.0$ and 10.0, heavy-heavy mesons have large discretization errors as these are governed by $pa \sim \alpha_s Ma$, so the corresponding data for Δ are not reliable. To summarize, the best estimate is $aM_b^0 = 2.31(12)$ obtained by matching M' to the pseudoscalar meson mass, $M_B = 5279$ MeV. Using M_{kin} instead of M' gives a consistent determination, $aM_b^0 = 2.21(22)$, though with larger errors.

A comparison of the three similar ways of determining M_b^0 using the Λ_h baryon mass is presented in Table V. Here, and in the following, we use the symbol Λ_h to represent a heavy-light-light Λ baryon with h labeling the heavy quark. Again, we find that the difference between the three methods are significant only for $aM^0 = 7.0$ and 10.0. Therefore, we determine M_b^0 by linearly interpolating the data at the lightest three M^0 values. The result is $aM_b^0 = 2.5(6)$ using $M_{\Lambda_b} = 5624$ MeV. This is consistent with the estimate from the meson sector; however, since it has much larger errors we do not consider it further.

The final issue in fixing aM_b^0 is related to the fact that our calculation fails to reproduce the experimental hyperfine splitting between the B and the B^*, as discussed in Sec. V D. Thus, it could be argued that determining aM_b^0 from the spin-averaged $1S$ mass $(m_B + 3m_{B^*})/4 = 5313$ MeV should give a better estimate. We find that $aM_b^0 = 2.32(12)$ obtained by matching M' to the spin-averaged mass is in complete agreement with the value obtained from m_B. Henceforth, we shall use the value $aM_b^0 = 2.32(12)$ for the b quark mass.

IV. MASS OF THE b QUARK, $m_{\overline{MS}}(m_{\overline{MS}})$

There are two steps needed to determine quark masses from lattice calculations. First, the bare quark masses have to be fixed by matching the lattice spectrum to experimental data. This has been described in Sec. III. Next, one needs to calculate the renormalization constants that relate these bare masses to the renormalized mass in the desired continuum scheme. The most common scheme is the modified minimal subtraction scheme ($\overline{MS}$) and we shall use it here. Standard continuum perturbation theory calculations can then be used to convert the result to any other scheme.

We calculate the $\overline{MS}$ mass by equating the pole mass on the lattice to that in the continuum:

$$m_{pole} = Z_m M_b^0 = Z_{cont}(\mu) m_{\overline{MS}}(\mu), \qquad (2)$$

where Z_m and Z_{cont} are the lattice and continuum renormalization constants [18], and μ is the scale at which the $\overline{MS}$ mass is defined. The perturbative series for both Z_m and Z_{cont} have renormalon ambiguities, therefore so does m_{pole}. However, in the desired relation,

$$m_{\overline{MS}}(\mu) = Z_{cont}^{-1}(\mu) Z_m M_b^0, \qquad (3)$$

$Z_{cont}^{-1} Z_m$ is ambiguity free.

We calculate m_{pole} on the lattice in two ways analogous to a previous determination using the Υ system [19]. In the first method, we use Eq. (1) and write $m_{pole} = M_{meson} - E_{sim} + E_0$ where M_{meson} is the experimental mass, E_{sim} is measured from the 2-point correlators, and E_0 is calculated

TABLE V. E_{sim} and Λ_h baryon masses in lattice units. Symbols have the same meaning as in Table IV.

	κ_l				κ_s			
aM^0	aE_{sim}	aM_{kin}	aM'	aM_{pert}	aE_{sim}	aM_{kin}	aM'	aM_{pert}
1.6	0.626(25)	2.19(31)	2.28(4)	2.27(5)	0.751(14)	2.54(16)	2.41(4)	2.39(4)
2.0	0.645(30)	2.56(40)	2.66(5)	2.67(4)	0.766(16)	2.93(20)	2.78(4)	2.79(3)
2.7	0.660(37)	3.21(53)	3.35(8)	3.34(5)	0.777(18)	3.62(29)	3.47(7)	3.46(3)
4.0	0.688(59)	4.7(11)	4.68(12)	4.59(12)	0.785(28)	5.02(50)	4.77(11)	4.69(9)
7.0	0.702(52)	9.2(11)		7.44(25)	0.783(28)	8.95(56)		7.52(23)
10.	0.726(72)	16.4(27)		10.2(4)	0.783(38)	14.2(14)		10.3(3)

TABLE VI. Results for the b quark pole and $\overline{MS}$ masses. Method 1 uses the meson mass and E_0, while method 2 uses Z_m and M_b^0. Both methods are described in more detail in [19]. The Direct method is described in the text. The first error quoted is statistical and includes interpolation-extrapolation to the physical quark masses; the second is due to the variation in the matching scale μ.

| Method to | Pole mass [GeV] | | $\overline{MS}$ mass [GeV] | | |
fix aM_b^0	Method 1	Method 2	Method 1	Method 2	Direct
M' (spin-avg B)	4.96(1)	4.97(10)	4.43(1)(4)	4.44(10)(4)	4.35(10)(4)
$M_{\text{kin}}(B)$	4.96(3)	4.76(41)	4.43(2)(4)	4.25(37)(4)	4.15(38)(4)

using perturbation theory. The second method, $m_{pole} = Z_m M_b^0$, uses the perturbative expression for Z_m. The quantities Z_m, and E_0, calculated to $O(\alpha_s)$, are listed in Table III for the different values of aM^0. The results for the two ways of fixing M_b^0 are given in Table VI.

This pole mass is converted, as in [20], to $m_{\overline{MS}}(\mu) = Z_{\text{cont}}^{-1}(\mu) m_{pole}$ using continuum perturbation theory for $Z_{\text{cont}}^{-1}(\mu)$ and the Brodsky-Lepage-Mackenzie procedure [21] to set the scale for the coupling constant. For μ we choose values between $1/a$ and π/a, avoiding those values where the BLM procedure fails. We then use 2-loop running to get the final result $m_{\overline{MS}}(m_{\overline{MS}})$, which, in principle, should not depend on the choice of the intermediate scale μ. These results are also given in Table VI, where the second error is the spread with respect to varying μ, and is indicative of the neglect of the higher order terms in the perturbative expressions.

Our preferred determination of $m_{\overline{MS}}(\mu)$ comes from "directly" expanding the product $Z_{\text{cont}}^{-1}(\mu) Z_m$ in Eq. (3) to $O(\alpha_s)$ [20] and using the Lepage-Mackenzie procedure [16] to calculate the appropriate scale q^* at which to evaluate α_s [20]. The reason for choosing this as the preferred method, as explained before, is the cancellation of renormalons in the product and the much better value of q^*. Continuum ($\overline{MS}$) running is then used to convert $m_{\overline{MS}}(\mu)$ to $m_{\overline{MS}}(m_{\overline{MS}})$. Our final result, obtained by fixing M_b^0 from the spin-averaged M', is

$$m_{\overline{MS}}(m_{\overline{MS}}) = 4.35(10)\binom{-3}{+2}(20) \text{ GeV}, \qquad (4)$$

where the first error includes statistics and interpolation uncertainty; the second is from the uncertainty in the lattice spacing; and the third is the systematic error associated with using one-loop perturbation theory. We estimate it as being $1 \times \alpha_s^2$. For typical values of α_s, depending on the matching scale μ, this is ~ 2.5–5 %. To be conservative, we assign a 200 MeV perturbative error to the mass.

There are two previous lattice determinations of m_b using a one-loop matching procedure. The NRQCD Collaboration [19,20,22] has calculated it within the Υ system, and the APE Collaboration [23,22] evaluates $E_{\text{sim}} - E_0$ for the B meson in the static theory. In addition, the APE group has recently extended their matching calculation to two loops [24]. These three results are

$$m_b^{\overline{MS}}(m_b^{\overline{MS}}) = 4.16(5)(15) \text{ GeV (NRQCD,1−loop)},$$

$$= 4.15(5)(20) \text{ GeV (APE,1−loop)},$$

$$= 4.41(5)(10) \text{ GeV (APE,2−loop)}. \qquad (5)$$

While all these results are consistent within errors, a couple of points are in order. First, the results of the APE calculation, which is similar to our method 1, suggest that the 2-loop term is large. This is consistent with our finding that the aq^* for E_0 (and Z_m) is small, ~ 0.6. Such a small value of aq^* is indicative of a large coefficient of the 2-loop term in the bubble summation approximation (BSA). Thus in methods 1 and 2, our estimate of perturbative uncertainty in the mass, due to the large value of $1 \times \alpha_s^2(q^*)$, is ~ 400 MeV. In our preferred direct method, $Z_{\text{cont}}^{-1}(\mu) Z_m$ has no renormalons, and the series is better behaved in the BSA. Our estimate of the perturbative uncertainty in the mass, 200 MeV, is based on the correspondingly larger value of q^*. To go beyond such an order of magnitude estimate, a two-loop calculation needs to be done within NRQCD since the 1-loop calculation shows a strong dependence of the coefficient on aM^0. Second, we find that the variation of $E_{\text{bind}} \equiv E_{\text{sim}} - E_0$ with aM^0 is small, i.e. $O(50)$ MeV (see Table XXII). We estimate that the $O(\Lambda_{QCD}^2/M)$ corrections to the APE results are of this order. Thus, we expect the systematic error in the APE calculation [24] to be slightly smaller than ours. We shall present a more detailed comparison of $m_{\overline{MS}}$ from the heavy-light and heavy-heavy systems on the same configurations in a separate publication [25].

V. HEAVY-LIGHT MESONS

The bare lattice results for meson energies and splittings as a function of κ and aM^0 are presented in Tables VII and VIII. These are first extrapolated-interpolated linearly to κ_l and κ_s, and then to aM_b^0 to obtain estimates for the physical states. (The data are not precise enough to include higher order corrections in the fits.) To show the dependence of the mass splittings on the heavy quark mass we plot them as a function of $1/\bar{M} \equiv 4/(3M_{H*} + M_H)$. In this paper, we use h to denote a generic heavy quark, H for a heavy-light meson, and an overbar for spin-averaged quantities. Where we find a significant $\bar{M}$ dependence, we quote the intercept (value in the static limit) and the slope. In cases where we find no significant slope, we do not show the corresponding fits in the figures. In general we find that the slope is $\sim \Lambda_{QCD}^2$, i.e.

TABLE VII. aE_{sim} for the $1S$ and $2S$ mesons is obtained using a two state fit, and $a(M_{H*}\text{-}M_H)$ is obtained from a fit to the ratio of the correlation functions. The splitting $a\Delta E(2S\text{-}1S)$ and the spin-averaged energy $\bar{E}=[3E_{\text{sim}}(H^*)+E_{\text{sim}}(H)]/4$ are calculated within the bootstrap process.

aM^0	κ	$aE_{\text{sim}}[1S(^1S_0)]$	$aE_{\text{sim}}[2S(^1S_0)]$	$a\Delta E(2S\text{-}1S)$	$a(M_{H*}\text{-}M_H)$	$a\bar{E}$
1.6	0.13690	0.493(03)	0.786(23)	0.293(24)	0.020(01)	0.508(03)
2.0		0.509(03)	0.795(23)	0.286(24)	0.017(01)	0.522(03)
2.7		0.522(03)	0.805(24)	0.283(25)	0.013(01)	0.532(03)
4.0		0.531(03)	0.818(24)	0.287(25)	0.009(01)	0.538(03)
7.0		0.534(04)	0.805(25)	0.271(26)	0.006(01)	0.538(04)
10.0		0.533(04)	0.800(26)	0.267(28)	0.004(01)	0.536(04)
1.6	0.13750	0.475(03)	0.770(27)	0.295(28)	0.020(01)	0.490(03)
2.0		0.491(03)	0.784(26)	0.293(27)	0.016(01)	0.503(03)
2.7		0.505(03)	0.797(29)	0.292(30)	0.013(01)	0.514(03)
4.0		0.514(04)	0.798(28)	0.284(30)	0.008(01)	0.520(04)
7.0		0.517(05)	0.792(28)	0.275(30)	0.005(01)	0.521(05)
10.0		0.517(05)	0.788(30)	0.272(33)	0.004(01)	0.520(05)
1.6	0.13808	0.459(04)	0.762(33)	0.303(34)	0.018(02)	0.472(04)
2.0		0.476(04)	0.777(35)	0.301(36)	0.015(02)	0.487(05)
2.7		0.490(05)	0.788(31)	0.298(32)	0.012(02)	0.499(05)
4.0		0.499(05)	0.800(38)	0.302(04)	0.008(01)	0.504(05)
7.0		0.501(05)	0.792(34)	0.292(36)	0.006(01)	0.505(05)
10.0		0.501(05)	0.786(35)	0.285(37)	0.004(01)	0.504(05)

the corrections to the static limit are $\sim$10% at M_b.

A summary of our results at the b mass is presented in Table IX and compared with experimental data in Fig. 3. We find that the radial and orbital splittings are in agreement with the preliminary experimental results. The hyperfine splittings $M_{B*}\text{-}M_B$ and $M_{B_s^*}\text{-}M_{B_s}$ are underestimated as will be discussed below. We are able to resolve the P state fine structure for the first time on the lattice; previous lattice calculations were done in the static limit and found no significant splittings [8,26]. There has been some controversy about the ordering of these states in potential model calculations [5]. We find that the B_0^* is the lightest and B_2^* is the heaviest. Details of the analyses follow.

In analyzing the mass splittings, we are motivated by the following qualitative picture; the mass of a heavy-light hadron is considered to be a sum of:

the pole mass of the heavy quark which is $\sim$1.5 GeV for the c quark and $\sim$5.0 GeV for the b;

the constituent mass m of the light quarks which is approximately 300 MeV for the u, d and 450 MeV for the s quark as inferred from the octet and decuplet light baryons, and which we expect to give the biggest contribution to the static binding energy of the ground-state hadrons;

an excitation energy of the light quark, which, for orbitally and radially excited states, we expect to be of the order of Λ_{QCD};

the $O(\Lambda_{QCD}^2/M_h)$ contributions due to the kinetic energy of the heavy quark and the heavy-light hyperfine energy $E_{\sigma_H\cdot\sigma_l}\approx 45$ MeV, inferred from the $B^*\text{-}B$ splittings;

TABLE VIII. aE_{sim} and splittings from fits to ratios of correlators for P states. To obtain the 2^+P states we spin-average over the $^3P_2(T)$ and $^3P_2(E)$ states.

aM^0	κ	$aE_{\text{sim}}(^3P_2T)$	$a\Delta E(^3P_2T\text{-}^3P_1)$	$a\Delta E(^3P_2T\text{-}^1P_1)$	$a\Delta E(^3P_2T\text{-}^3P_0)$	$a\Delta E(^3P_2T\text{-}^3P_2E)$
1.6	0.13690	0.769(08)	0.042(11)	0.028(07)	0.082(11)	0.020(14)
2.0		0.774(06)	0.042(11)	0.028(07)	0.078(11)	0.020(14)
2.7		0.772(04)	0.042(11)	0.028(07)	0.073(11)	0.020(13)
1.6	0.13750	0.760(09)	0.048(13)	0.032(09)	0.087(12)	0.025(16)
2.0		0.765(07)	0.048(13)	0.032(08)	0.083(12)	0.025(16)
2.7		0.765(11)	0.048(13)	0.032(08)	0.078(12)	0.025(15)
1.6	0.13808	0.752(10)	0.056(16)	0.037(10)	0.093(14)	0.030(20)
2.0		0.757(08)	0.055(16)	0.036(10)	0.088(14)	0.029(19)
2.7		0.757(12)	0.055(15)	0.036(10)	0.083(14)	0.028(19)

TABLE IX. Mass estimates in MeV for various meson states. The b quark mass is fixed using the spin-averaged $\bar{B}(1S)$. The first error in the lattice data is statistical (including the statistical error in the lattice spacing), the second comes from varying a^{-1} between 1.8 and 2.0 GeV, and for the strange mesons, the third error comes from the uncertainty in setting the strange quark mass. Finite lattice volume effects, which could be large for the excited states, have not been addressed in this exploratory study. Preliminary experimental values are denoted by asterisks. The lattice results quoted against the B_J^* and B_{sJ}^* states correspond to the spin-average of the respective P states, and the experimental numbers are for the unresolved broad resonances. Unless stated otherwise, experimental numbers are from the Particle Data Book [22].

State	($n\,J^P$)	Lattice MeV	Expt. MeV
		Heavy-light mesons	
B	$1(0^-)$	$5296(04)(^{-2}_{+3})$	5279
	$2(0^-)$	$5895(116)(^{+20}_{-32})$	5860(*)
B^*	$1(1^-)$	$5319(02)(^{+0}_{-2})$	5325(1)
B_0^*	$1(0^+)$	$5670(37)(^{+16}_{-24})$	
B_J^*		$5770(31)(^{+24}_{-35})$	5697(9)
B_2^*	$1(2^+)$	$5822(45)(^{+27}_{-35})$	5779(*) [27]
			5725–5768(*) [28]
		Heavy-strange mesons	
B_s	$1(0^-)$	$5385(15)(^{-6}_{+7})(^{+20}_{-0})$	5369(2)
	$2(0^-)$	$5935(57)(^{+27}_{-38})(^{+9}_{-0})$	
B_s^*	$1(1^-)$	$5412(14)(^{-4}_{+2})(^{+20}_{-0})$	5416(3)
B_{s0}^*	$1(0^+)$	$5742(27)(^{+14}_{-20})(^{+15}_{-0})$	
B_{sJ}^*		$5836(25)(^{+20}_{-28})(^{+14}_{-0})$	5853(15)
B_{s2}^*	$1(2^+)$	$5878(26)(^{+23}_{-33})(^{+11}_{-0})$	

and a residual binding energy E_{be} encapsulating the remaining interactions which we expect to be small $[O(\Lambda_{QCD}^3/M_h^2)]$.

We accordingly construct different linear combinations of meson and baryon masses to isolate individual terms and estimate their size and dependence on the quark masses.

A. B_s-B_d splitting

The spin-averaged splitting between B_s and B_d mesons should be dominated by the difference of the strange and light quark masses. Our estimate is $\bar{M}_{B_s}-\bar{M}_{B_d} = 90(9)(^{+5}_{-3})(^{+20}_{-0})$ MeV, to be compared to the experimental value 91(3) MeV. The largest uncertainty, the third error, comes from setting κ_s; estimates using $\kappa_s(M_{K*})$ are $\sim 20\%$ higher, a feature seen in all quenched calculations.

Previous calculations have reported the following results for $M_{B_s}-M_{B_d}$: $87(^{+15}_{-12})(^{+6}_{-12})$ MeV [29], $86(12)(^{+7}_{-9})$ MeV [30], and $107(13)$ MeV [31]. The JLQCD calculation [32], done at $\beta = 5.7$, 5.9, and 6.1, sees indications of $\sim 20\%$ scaling violations between $\beta = 5.9$ and 6.1. Averaging the data at the largest two β they find $87(7)(4)(^{+19}_{-0})$ MeV. For comparison, our result is $87(9)(^{+5}_{-3})(^{+19}_{-0})$ MeV, and the experimental value 90(2) MeV [22].
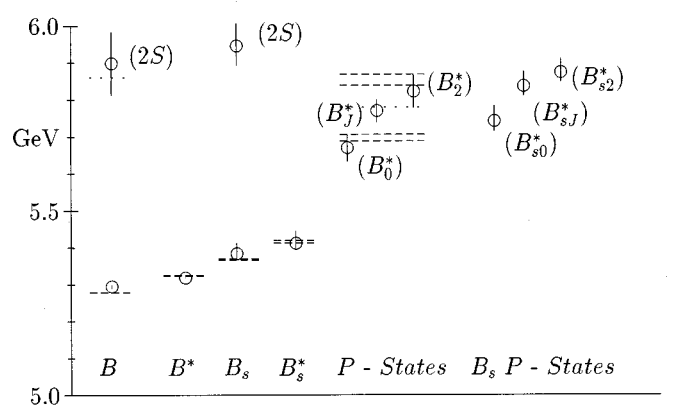

FIG. 3. Overview of the B meson spectrum. Circles denote lattice results, dashed lines give the range of experimental values [22], and the dotted lines indicate preliminary experimental estimates [27]. Errors include statistics and the uncertainty in κ_s. Uncertainty due to the variation of a^{-1} between 1.8 and 2.0 GeV is not included.

In our picture, the heavy quark mass dependence should result from the difference of the kinetic and hyperfine energies of the heavy quark in B_s and B_d mesons. (In the spin-averaged splitting, $\bar{M}_{B_s}$-$\bar{M}_{B_d}$, only the difference of the kinetic energies remains.) Therefore, we expect this splitting to be independent of the heavy quark mass up to terms of $O((m_s$-$m_d)/M)$. The experimental data show a $\sim 10\%$ increase going from the B to the D meson. Our data, given in Table X, show no significant dependence on the heavy quark mass; however, as shown in Fig. 4, they are consistent with the experimental trend. This consistency has also been found in Ref. [13], where the heavy quark mass dependence has been studied at higher statistics and for a heavy quark mass range between the b and the c.

B. $2S$-$1S$ splitting

The raw data for the $2\,^1S_0$-$1\,^1S_0$ splitting are given in Table VII, and after extrapolation or interpolation to κ_l and κ_s, in Table XI. This splitting should be dominated by the difference in the kinetic energies of the light and the heavy quarks which give contributions of $O(\Lambda_{QCD}^2/m_{constituent})$ and

TABLE X. Spin-averaged H_s-H_d splitting as a function of M^0. The experimental value is 96(6) MeV.

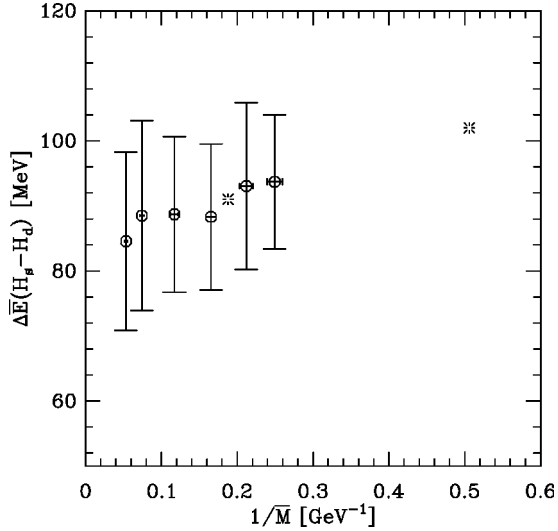|	$\Delta E(\bar{H}_s$-$\bar{H}_d)$			
	Lattice units		MeV	
aM^0	$\kappa_s(m_K)$	$\kappa_s(m_{K*})$	$\kappa_s(m_K)$	$\kappa_s(m_{K*})$
1.6	0.046(06)	0.060(09)	94(10)	114(14)
2.0	0.049(07)	0.059(10)	93(13)	114(17)
2.7	0.046(06)	0.056(08)	88(11)	108(14)
4.0	0.046(07)	0.057(09)	89(12)	108(15)
7.0	0.046(08)	0.056(11)	89(15)	108(18)
10.0	0.044(07)	0.054(09)	85(14)	103(16)

FIG. 4. Spin-averaged H_s-H_d splitting as a function of the inverse spin-averaged meson mass $\bar{M}$. The bursts denote the experimental values for B and D mesons.

FIG. 5. $2S$-$1S$ splitting for $^1S_0$ states as a function of the inverse spin-averaged meson mass. The burst denotes the preliminary $^1S_0$ experimental value [27].

$O(\Lambda^2_{\mathrm{QCD}}/M)$ respectively. With our data, as shown in Table XI and illustrated in Fig. 5, we cannot resolve any dependence on either the light or the heavy quark mass. Our results for B and B_s systems are $602(86)(^{+25}_{-35})$ and $559(55)(^{+31}_{-38})(^{+0}_{-12})$ MeV respectively, to be compared with the preliminary experimental value, 581 MeV, for the B [27]. In the charm sector, the most relevant experimental value is 627 MeV for the $D^{*\prime}$ [33].

We do not give results for the spin-averaged splitting $2\bar{S}$-$1\bar{S}$, since the signal for the $^3S_1$ excited state is less reliable than that for the $^1S_0$.

C. $1P$-$1S$ splitting

The two main contributions to the spin-averaged $1P$-$1S$ splitting should be the energy it takes to excite the light quark to angular momentum one, $O(\Lambda_{\mathrm{QCD}})$, and the difference of the kinetic energy of the heavy quark in an S-wave and a P-wave light quark background, $O(\Lambda^2_{\mathrm{QCD}}/M)$. Our results, shown in Table XII, are constructed from the raw data given in Tables VII and VIII. Our estimates are $457(31)(^{+24}_{-35})$ MeV for the B, and $428(27)(^{+27}_{-41})(^{+0}_{-2})$ MeV for the B_s.

Experimentally the P states have not been resolved. The P wave resonances $B^*_J(5732)$ (or B^{**}) at 5697(9) MeV and $B^*_{s,J}(5850)$ at 5853(15) MeV are expected to be a superposition of the various P states. These are 419 and 484 MeV higher than the corresponding $^1S_0$ states. We use them as estimates of the spin-averaged $1P$-$1S$ splittings to compare against.

The variation with either the heavy or the light quark mass is similar to that in the $2S$-$1S$ splitting. There is a small decrease with increasing light quark mass. The slope, as a function of $1/\bar{M}$, is $0.380(202)(^{+53}_{-66})(^{+68}_{-0})$ GeV^2 for κ_l, and an almost identical value at κ_s, as shown in Fig. 6.

D. B^*-B splitting

Our results for the hyperfine splitting are shown in Table XIII and plotted in Fig. 7. A linear fit to the B_d data gives $0.138(38)(^{+11}_{-17})$ GeV^2 for the slope and $-2(7)$ MeV for the intercept at infinite mass. A zero intercept is consistent with the heavy quark effective theory (HQET) picture in which the B^*-B splitting comes from the interaction of the heavy quark spin with the color field, i.e., through a $\sigma \cdot B/(2M)$

TABLE XI. $2S$-$1S$ splittings extrapolated-interpolated to κ_l and κ_s. The preliminary experimental result for B_d is 581 MeV [27], while for B_s there is no result as yet.

| | $\Delta E(2\,^1S_0$-$1\,^1S_0)$ | | | | | |
| | Lattice units | | | MeV | | |
aM^0	κ_{light}	$\kappa_s(m_K)$	$\kappa_s(m_{K*})$	κ_{light}	$\kappa_s(m_K)$	$\kappa_s(m_{K*})$
1.6	0.310(49)	0.297(27)	0.294(24)	593(92)	570(53)	564(49)
2.0	0.315(54)	0.294(27)	0.289(24)	603(101)	563(54)	553(50)
2.7	0.313(46)	0.292(27)	0.287(25)	600(91)	560(55)	551(53)
4.0	0.305(59)	0.291(30)	0.287(26)	585(114)	558(60)	551(54)
7.0	0.307(53)	0.280(29)	0.274(27)	588(103)	537(60)	525(57)
10.0	0.299(53)	0.275(31)	0.270(29)	574(103)	527(64)	517(62)

TABLE XII. Spin-averaged P-S splittings.

| | $\Delta E(\bar{P}\text{-}\bar{S})$ | | | | | |
| | Lattice units | | | MeV | | |
aM^0	κ_{light}	$\kappa_s(m_K)$	$\kappa_s(m_{K*})$	κ_{light}	$\kappa_s(m_K)$	$\kappa_s(m_{K*})$
1.6	0.251(13)	0.238(08)	0.235(08)	481(29)	457(23)	451(23)
2.0	0.244(13)	0.230(07)	0.227(07)	467(27)	442(21)	436(23)
2.7	0.232(24)	0.219(08)	0.216(07)	446(49)	420(23)	414(23)

TABLE XIII. H^*-H splitting as a function of M^0. The experimental results are 45.78(35) MeV for B_d and 47.0(2.6) MeV for B_s.

| | $\Delta E(H^*\text{-}H)$ | | | | | |
| | Lattice units | | | MeV | | |
aM^0	κ_{light}	$\kappa_s(m_K)$	$\kappa_s(m_{K*})$	κ_{light}	$\kappa_s(m_K)$	$\kappa_s(m_{K*})$
1.6	0.017(03)	0.019(01)	0.020(01)	32(05)	37(03)	38(03)
2.0	0.014(02)	0.016(01)	0.016(01)	27(05)	31(03)	32(02)
2.7	0.011(02)	0.012(01)	0.013(01)	21(05)	24(03)	25(02)
4.0	0.007(02)	0.008(01)	0.008(01)	13(04)	16(02)	16(02)
7.0	0.005(02)	0.006(01)	0.006(01)	10(03)	11(02)	11(02)
10.0	0.004(02)	0.004(01)	0.004(01)	8(04)	8(02)	8(02)

interaction. Our estimates are $24(5)\binom{+2}{-3}$ MeV and $27(3)\binom{+2}{-3}\binom{+1}{-0}$ MeV for the B and the B_s respectively, and $\Delta E(B_s^* - B_s)/\Delta E(B_d^* - B_d) = 1.19(20)\binom{-2}{+2}\binom{+4}{-0}$. These splittings are roughly half the experimental values, 46 and 47 MeV respectively.

An underestimate of hyperfine splittings has also been seen by the previous quenched calculations [29,10,34,31,32]. The results of the JLQCD calculation [32] suggest that this is not due to scaling violations. Present preliminary unquenched calculations [35] do not show any significant improvement either, however, the mass of the two flavors of dynamical quarks is large, $\sim m_s$. Further work is needed to clarify this issue.

All hyperfine splittings, including those in the P state and baryon sector, are, to leading order, generated by the $\sigma \cdot B$ term in the quark action. It has recently been pointed out that the coefficient of this term should be larger by a factor of 1.15–1.30 [35,36]. Such a correction would bring the quenched results much closer to the experimental values.

E. P fine structure

In the jj coupling scheme there are two doublets of P states which are distinguished by the angular momentum of the light quark: $j_l = 1/2$ and $j_l = 3/2$. The states in each doublet are separated by a spin flip of the heavy quark into a 0^+
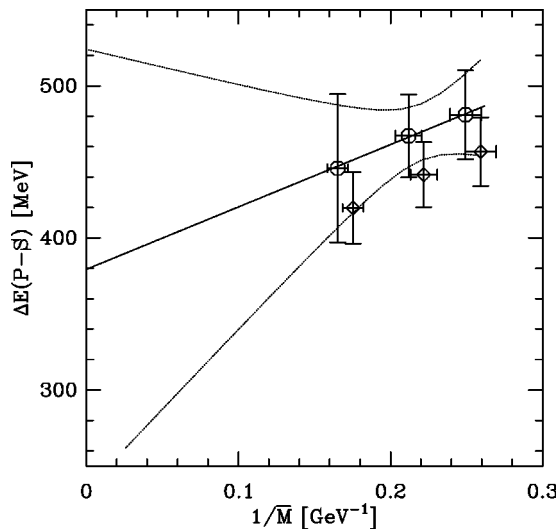
and a 1^+ state for $j_l = 1/2$ (B_0^* and B_1^*), and a $1^{+\prime}$ and a 2^+ state for $j_l = 3/2$ (B_1 and B_2^*). We therefore expect the spin-averages of the $j_l = 3/2$ and the $j_l = 1/2$ doublets to be separated by $O(\Lambda_{QCD})$, and the states within each doublet by $O(\Lambda_{QCD}^2/M)$.

The experimental situation is as follows. There exists a broad resonance at 5697(9) MeV [22], whose spin has not been determined and which is believed to be a superposition of various P states. There is also a preliminary experimental result by the DELPHI Collaboration [27] for a narrow P state which is 81 MeV heavier than this resonance. Its spin is also not resolved, but it is believed to be either $J=1$ or $J=2$.

Recently, estimates for individual P states have been obtained by fitting the line shape of the broad resonance using phenomenological input based on HQET for the mass splittings, decay widths, relative production rates, and branching fractions [28]. Using this method, the CDF and ALEPH Collaborations obtain a mass of the B_2^* of $\sim$5730 MeV. This result seems to be rather insensitive to the assumption about

FIG. 6. Spin-averaged P-S splitting of the H_d (circles) and H_s mesons (diamonds) as a function of the inverse spin-averaged meson mass. The lines denote a linear fit to the H_d data.
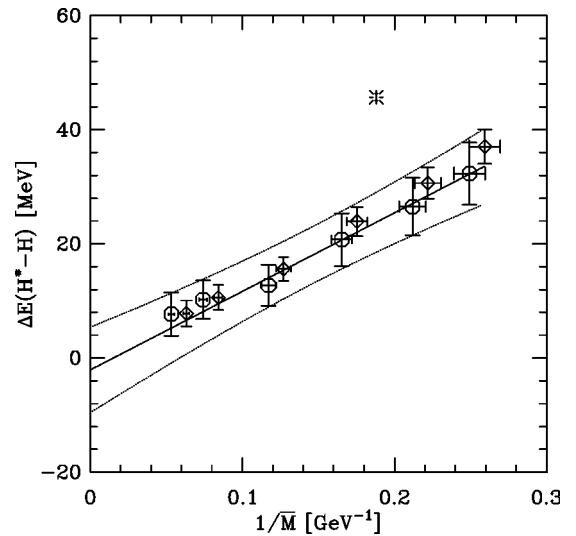

FIG. 7. Hyperfine splitting as a function of the inverse spin-averaged meson mass. Circles denote the splitting for H_d mesons, diamonds, for H_s mesons. For clarity, the diamonds are shifted to the right. The burst denotes the experimental value for H_d mesons. The lines are a linear fit to the H_d data.

TABLE XIV. H_2^*-H_0^* splittings.

	$\Delta E(H_2^*$-$H_0^*)$					
	Lattice units			MeV		
aM^0	κ_{light}	$\kappa_s(m_K)$	$\kappa_s(m_{K*})$	κ_{light}	$\kappa_s(m_K)$	$\kappa_s(m_{K*})$
1.6	0.088(17)	0.078(11)	0.075(11)	168(32)	149(23)	144(22)
2.0	0.083(17)	0.073(11)	0.071(11)	159(32)	140(22)	136(21)
2.7	0.078(16)	0.068(11)	0.066(10)	150(32)	131(22)	127(21)

the B_2^*-B_1^* splitting, which the phenomenological model predicts to be $\sim$100 MeV. The *L*3 Collaboration also uses hyperfine splittings of 12 MeV as input, but makes no assumption about the splitting between the j_l=3/2 and the j_l=1/2 doublet, and obtains slightly higher masses, B_2^* $\sim$5768 and $B_1^*$$\sim$5670 MeV. Our resolution of the *P* state fine structure is as follows.

First, we discuss the 0^+ and 2^+ states for which the data are shown in Table XIV and Fig. 8. We find that B_2^*-B_0^*=155(32)$\binom{+9}{-13}$ MeV and B_{s2}^*-B_{s0}^*=136(23)$\binom{+10}{-13}\binom{+0}{-4}$ MeV. At κ_l, the slope versus $1/\bar{M}$ is 0.224(70)$\binom{+20}{-27}$ GeV^2 and the intercept is 112(33)$\binom{+5}{-6}$ MeV. For B_s *P* states, the slope is 0.209(45)$\binom{+19}{-26}\binom{+0}{-4}$ GeV^2 and the intercept is 97(23)$\binom{+5}{-8}\binom{+0}{-4}$ MeV. These results are a significant improvement over previous values obtained in the static approach, i.e. $\sim$50(100) MeV [26] and $\sim$80(75) MeV [8] for the intercept.

The situation in model calculations is very unclear. The predictions are model dependent, and details like the treatment and the mass of the light quark are significant [5]. At this point there is no consensus on even the sign of the splitting.

To study the J=1 states we used operators with $^3P_1$ and $^1P_1$ quantum numbers in the *LS* coupling scheme as defined
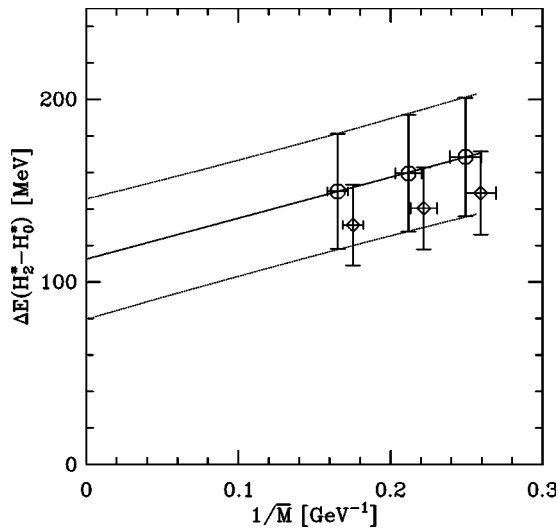

FIG. 8. H_2^*-H_0^* (denoted by octagons) and H_{s2}^*-H_{s0}^* (the diamonds are shifted by 0.01 in the x direction for clarity) splittings as a function of the inverse spin-averaged meson mass. A linear fit to H_2^*-H_0^* is also shown.

in Table II. The corresponding correlation functions get contributions from both the physical states. Therefore, at large Euclidean times both correlators are dominated by the same lowest state. The masses we extract from short Euclidean time ($\Delta Et \ll 1$) correspond to unmixed states in the *LS* scheme and are not the physical masses [37]. To get the latter requires a signal in the mixed correlators followed by a diagonalization of the 2×2 matrix. Unfortunately, our data does not show a signal in the mixed correlators, and therefore we do not have results for the physical J=1 states. The numbers presented in Table IX under 1^+ are those obtained using the $^3P_1$ correlators. Estimates obtained from the $^1P_1$ correlators are almost identical to the center of mass of the ^3P states.

VI. HEAVY-LIGHT-LIGHT BARYONS

The heavy-light-light baryons, in the heavy quark limit, can be classified according to the angular momentum of the light quarks. At zero orbital angular momentum, the light quarks can have total spin s_1=0 (anti-symmetric in both spin and flavor) and s_l=1 (symmetric in both). As summarized in Table XVI, there are three states with s_l=0; *udb*, *usb*, and *dsb* which are called the Λ_b^0, Ξ_b^0 and Ξ_b^- baryons with total spin 1/2. The system with s_l=1 splits up into six hyperfine doublets, each containing states with spin 1/2 and spin 3/2. These six doublets are $(\Sigma_b^+, \Sigma_b^{*+})$, $(\Sigma_b^0, \Sigma_b^{*0})$, $(\Sigma_b^-, \Sigma_b^{*-})$, $(\Xi_b^{\prime 0}, \Xi_b^{*0})$, $(\Xi_b^{\prime -}, \Xi_b^{*-})$, and $(\Omega_b^-, \Omega_b^{*-})$ [4]. The pairs of states $(\Sigma_b^0, \Lambda_b^0)$, and $(\Xi_b^\prime, \Xi_b)$, do not mix if flavor SU(2) is unbroken. We ensure this in our lattice calculation by only analyzing baryons with degenerate combinations of light quarks. The raw data are given in Table XV. Baryons with a generic heavy quark are denoted as Λ_h, Σ_h etc. To get *us* and *ds* combinations we extrapolate linearly in the degenerate light quark mass to the average mass $(m_s+m_l)/2$, which we label κ_{av}. A summary of the experimental numbers and our lattice results is given in Table XVI and shown in Fig. 9.

The UKQCD Collaboration has previously presented a similarly detailed analysis of the baryon spectrum [9]. They used the tree-level clover action (C_{SW}=1) at β=6.2 [$1/a$=2.9(2) GeV] and four heavy κ around the charm quark mass. In contrast to our calculation, their *b* spectrum was obtained by extrapolation in $1/M$. To facilitate comparison, we summarize their results in Table XVI. Within errors these are consistent with our findings, although our results are slightly higher and have a slightly smaller light quark mass

TABLE XV. E_{sim} values for Λ_h, Σ_h, and Σ_h^* baryons, and Σ_h^*-Σ_h splittings from ratio fits.

aM^0	κ	$aE_{\mathrm{sim}}(\Lambda_h)$	$aE_{\mathrm{sim}}(\Sigma_h)$	$aE_{\mathrm{sim}}(\Sigma_h^*)$	$a\Delta E(\Sigma_h^*\text{-}\Sigma_h)$
1.6	0.13690	0.801(10)	0.852(10)	0.869(10)	0.014(02)
2.0		0.813(11)	0.869(11)	0.883(10)	0.011(02)
2.7		0.823(14)	0.884(12)	0.894(10)	0.008(02)
4.0		0.823(20)	0.899(14)	0.907(14)	0.005(01)
7.0		0.816(29)	0.916(20)	0.921(21)	0.004(01)
10.0		0.806(40)	0.929(30)	0.931(32)	0.003(01)
1.6	0.13750	0.756(12)	0.822(12)	0.838(12)	0.014(02)
2.0		0.769(14)	0.838(13)	0.851(13)	0.011(02)
2.7		0.781(17)	0.852(14)	0.860(11)	0.008(02)
4.0		0.787(27)	0.866(16)	0.875(19)	0.005(02)
7.0		0.782(41)	0.888(23)	0.895(25)	0.004(01)
10.0		0.776(56)	0.907(35)	0.912(38)	0.003(01)
1.6	0.13808	0.710(17)	0.795(13)	0.812(15)	0.015(03)
2.0		0.726(20)	0.811(14)	0.825(15)	0.011(02)
2.7		0.739(25)	0.826(17)	0.829(13)	0.008(02)
4.0		0.755(41)	0.835(22)	0.843(19)	0.005(02)
7.0		0.758(32)	0.865(29)	0.876(34)	0.004(02)
10.0		0.766(43)	0.894(43)	0.900(45)	0.002(02)

FIG. 9. Overview of the b baryon spectrum. Circles denote our lattice results, dashed lines give experimental error bounds [22], and dotted lines show preliminary experimental results [3,27].

dependence. An important point, as discussed below, is that we are able to resolve hyperfine splittings for the first time.

The baryon splittings are also analyzed using the phenomenological model discussed in Sec. V. In heavy-light-light baryons there is an additional light-light hyperfine interaction ($E_{\sigma_l \cdot \sigma_l}$), which is expected to be of order Λ_{QCD}.

A. Λ-$\bar{B}$ splitting

We first consider the splitting $M_{\Lambda_h}-(M_H+3M_{H^*})/4$. In this combination, the heavy quark mass cancels and there is no contribution from the hyperfine interaction $E_{\sigma_H \cdot \sigma_l}$. Since

the light quarks are in a ground state with total spin zero, the mass of the extra light quark in the baryon gives the dominant contribution. This is borne out by the experimental values: 311(10) and 310(2) MeV for the b and c systems respectively, indicating the absence of $O(\Lambda_{\mathrm{QCD}}^2/M)$ contributions from the difference in kinetic energy to the splitting (see Fig. 1). Our lattice data, displayed in Table XVII, show little dependence on the heavy quark mass, Fig. 10. The variation with the light quark mass is linear as expected, see Fig. 11. Our estimates are Λ_b-$\bar{B}=370(67)(^{+14}_{-20})$ MeV and Ξ_b-$\bar{B}_s$ $=392(50)(^{+15}_{-0})$ MeV.

There exist a number of previous results for Λ_b-B, obtained by extrapolating in the heavy quark mass, $359(^{+55}_{-45})(^{+27}_{-26})$ MeV [9] and 458(144)(18) MeV [39]; in the static limit, $420(^{+100}_{-90})(^{+30}_{-30})$ MeV [29]; and with NRQCD on

TABLE XVI. Summary of masses in GeV for baryons with quark content shown in column two [h denotes a generic heavy quark (c or b), l stands for a u or d quark]. Errors are as explained in the caption to Table IX. Finite lattice volume effects, which could be large, have not been addressed in this exploratory study. Experimental results are given in columns three and four. Previous results (UKQCD [9]) are in column five. The last column gives results of our calculation.

Baryon	Quark content	Experimental		[9]	Our results
		c	b	b	b
		Λ-like ($s_l=0$, $j=1/2$)			
Λ_h	(udh)	2.285(1)	5.624(9)	$5.64(^{+5}_{-5})(^{+3}_{-2})$	$5.679(71)(^{+14}_{-19})$
Ξ_h	(lsh)	2.466		$5.76(^{+3}_{-5})(^{+4}_{-3})$	$5.795(53)(^{+9}_{-15})(^{+15}_{-0})$
		Σ-like ($s_l=1$, $j=1/2$)			
Σ_h	(llh)	2.453(1)	5.797(8) [3]	$5.77(^{+6}_{-6})(^{+4}_{-4})$	$5.887(49)(^{+25}_{-37})$
Ξ_h'	(lsh)	2.574 [28]		$5.90(^{+6}_{-6})(^{+4}_{-4})$	$5.968(39)(^{+20}_{-32})(^{+24}_{-0})$
Ω_h	(ssh)	2.704(4)		$5.99(^{+5}_{-5})(^{+5}_{-5})$	$6.048(33)(^{+16}_{-26})(^{+34}_{-0})$
		Σ^*-like ($s_l=1$, $j=3/2$)			
Σ_h^*	(llh)	2.519(2)	5.853 [3]	$5.78(^{+5}_{-6})(^{+4}_{-3})$	$5.909(47)(^{+25}_{-39})$
Ξ_h^*	(lsh)	2.645		$5.90(^{+4}_{-6})(^{+4}_{-5})$	$5.989(39)(^{+22}_{-34})(^{+25}_{-0})$
Ω_h^*	(ssh)			$6.00(^{+4}_{-5})(^{+5}_{-5})$	$6.069(34)(^{+18}_{-30})(^{+35}_{-0})$

TABLE XVII. Splitting between the Λ_h and the spin-averaged H. The experimental value for the Λ_H-$\bar{B}_d$ is 311(10) MeV.

	$\Delta E(\Lambda_h$-$\bar{H})$					
	Lattice units			MeV		
aM^0	κ_{light}	$\kappa_s(m_K)$	$\kappa_s(m_{K*})$	κ_{light}	$\kappa_s(m_K)$	$\kappa_s(m_{K*})$
1.6	0.187(25)	0.263(13)	0.280(15)	359(52)	504(27)	536(22)
2.0	0.191(30)	0.263(14)	0.280(15)	367(60)	505(31)	535(25)
2.7	0.194(38)	0.264(18)	0.280(18)	372(76)	506(38)	536(31)
4.0	0.215(59)	0.266(28)	0.278(22)	414(116)	510(59)	532(45)
7.0	0.228(52)	0.263(28)	0.271(30)	438(104)	505(60)	520(60)
10.0	0.252(72)	0.264(38)	0.267(41)	484(144)	507(79)	513(82)

coarse lattices 363(9) MeV [31] (no systematic errors quoted). These values are consistent with our result Λ_b-B $= 388(68)(^{+15}_{-23})$ MeV.

B. $\bar{\Sigma}$-Λ splitting

In our picture, the splitting $(2\Sigma_h + 4\Sigma_h^*)/6$-$\Lambda_h$ depends on $E_{\sigma_l \cdot \sigma_l}$, the hyperfine interaction between the light quarks, the difference of the binding energies, and of the kinetic energies of the heavy quark in each baryon. Experimentally, it is found to be independent of the heavy quark mass: $(2\Sigma_c + 4\Sigma_c^*)/6$-$\Lambda_c = 212$ MeV and the preliminary estimate $(2\Sigma_b + 4\Sigma_b^*)/6$-$\Lambda_b = 210$ MeV (see also Fig. 1). These numbers are roughly 2/3 of the delta-nucleon splitting (293 MeV). Such a ratio is obtained in a simple non-relativistic model where these splittings are dominated by the light quark hyperfine interaction. The lattice results shown in Table XVIII and Fig. 12 are also independent of the heavy quark mass and give $221(71)(^{+12}_{-16})$ MeV at M_b.

In the charmed sector the experimental value changes significantly on replacing d with s, i.e. $(2\Xi_c' + 4\Xi_c^*)/6$-Ξ_c $= 154$ MeV. Our lattice results at the b mass also show a decrease with $221(71)(^{+12}_{-16})$ going to $186(51)(^{+13}_{-17})(^{+0}_{-10})$ MeV, although the difference is not statistically significant.

The UKQCD Collaboration [9] reports Σ_b-Λ_b $= 190(^{+60}_{-75})(^{+30}_{-30})$ MeV and Ξ_b'-$\Xi_b = 157(^{+52}_{-64})(^{+11}_{-11})$ MeV

from extrapolating in the heavy quark mass to the b. Our results for these splittings are 209(71) and $177(54)(^{+0}_{-10})$ MeV respectively.

The Σ_h^*-Σ_h splitting should depend only on the heavy-light hyperfine interaction $E_{\sigma_h \cdot \sigma_l}$. It is therefore expected to be proportional to $1/M_h$. Our lattice results, shown in Table XIX, resolve these splittings for the first time. A linear fit to the three lightest $\bar{M}$ values that bracket M_b^0 gives $-17(11)(^{+0}_{-1})$ MeV for the intercept and $0.188(44)(^{+17}_{-22})$ GeV^2 for the slope. However, as apparent from Fig. 13, if the fit is constrained to have zero intercept, then it would have a much smaller slope. Based on the assumption that the wave-function at the origin is similar, one expects the slope for the baryon splitting to be 0.75 that for mesons [38], which was found to be $0.138(38)(^{+11}_{-17})$ GeV^2 in Sec. V D. This expectation does not hold in the charm sector where Σ_c^*-Σ_c ≈ 66 MeV whereas D^*-$D \approx 140$ MeV.

The preliminary experimental value is Σ_b^*-Σ_b $= 56(8)$ MeV [3]. It is however likely that at least one of the states has been misidentified [4], and this number is too large. Scaling the experimental value Σ_c^*-$\Sigma_c = 66$ MeV by
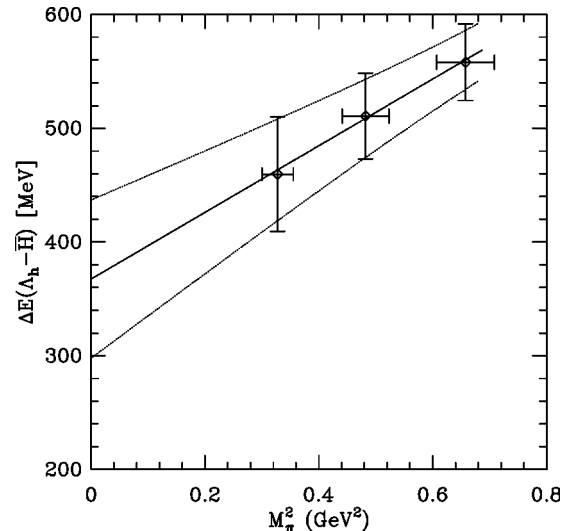

FIG. 11. Spin-averaged Λ_h-H splitting as a function of the light quark mass represented by the corresponding pseudoscalar meson mass squared M_π^2.

FIG. 10. Spin-averaged Λ_h-H splitting as a function of $1/\bar{M}$.

TABLE XVIII. Splitting between the spin-averaged Σ_h and Λ_h as a function of M^0. κ_{av} corresponds to setting the light quark mass to $(m_s + m_l)/2$. The preliminary experimental value is $\bar{\Sigma}_b - \Lambda_b = 210$ MeV [3].

	$\Delta E(\bar{\Sigma}_h - \Lambda_h)$									
	Lattice units					MeV				
aM^0	κ_{light}	$\kappa_{av}(m_K)$	$\kappa_{av}(m_{K*})$	$\kappa_s(m_K)$	$\kappa_s(m_{K*})$	κ_{light}	$\kappa_{av}(m_K)$	$\kappa_{av}(m_{K*})$	$\kappa_s(m_K)$	$\kappa_s(m_{K*})$
1.6	0.124(29)	0.102(21)	0.097(19)	0.080(14)	0.070(14)	237(55)	196(41)	186(39)	154(29)	135(29)
2.0	0.119(34)	0.099(25)	0.095(23)	0.080(17)	0.071(15)	227(65)	190(48)	182(46)	153(33)	137(32)
2.7	0.106(38)	0.092(28)	0.089(26)	0.078(18)	0.072(16)	204(72)	177(53)	171(50)	150(36)	138(33)
4.0	0.092(59)	0.088(44)	0.087(40)	0.084(29)	0.082(23)	176(112)	169(83)	167(77)	161(56)	157(45)
7.0	0.126(56)	0.118(39)	0.116(37)	0.110(31)	0.106(32)	241(108)	226(76)	223(71)	211(59)	204(62)
10.0	0.141(79)	0.135(53)	0.134(49)	0.129(42)	0.127(45)	270(152)	259(102)	257(95)	248(81)	243(89)

M_c/M_b suggests ~ 20 MeV for this splitting [4,40]. We find $\Sigma_b^* - \Sigma_b = 19(7)\binom{+2}{-3}$ MeV; however this could be an underestimate based on the general discussion of hyperfine interactions in Sec. V D.

The raw lattice data does not show a dependence on the light quark mass. Experimentally, there exists data for strange baryons only in the c sector. The preliminary estimate $\Xi_c^* - \Xi_c' \approx 77$ MeV is ≈ 11 MeV larger than the $\Sigma_c^* - \Sigma_c$ splitting. At the b, heavy quark scaling suggests that this difference should be reduced by the factor $M_c/M_b \approx 0.3$, making it much smaller than our resolution. We find $\Xi_b^* - \Xi_b' = 19(5)\binom{+2}{-3}$ and $\Omega_b^* - \Omega_b = 18(4)\binom{+2}{-3}$ MeV.

VII. HEAVY-HEAVY-LIGHT BARYONS

It is theoretically interesting to study heavy-heavy-light baryons even though it is exceedingly hard to produce two overlapping b quarks in experiments. The two heavy quarks are expected to bind in a color anti-triplet state whose size is much smaller than Λ_{QCD}. It thus interacts with the light degrees of freedom to yield a level structure similar to that of heavy-light mesons [41,42].

In the S-wave baryons, the total angular momentum of the two heavy quarks is $J=0$ or 1. For identical quarks only $J=1$ is possible. There are two different ways to couple the light quark spin to this configuration. The $J=3/2$ states are denoted as Ξ_{bb}^{*0}, Ξ_{bb}^{*-}, and Ω_{bb}^{*-}, and the $J=1/2$ states as Ξ_{bb}^0, Ξ_{bb}^-, and Ω_{bb}^- (the quark content is bbu, bbd, and bbs respectively). These are split by a heavy-light hyperfine in-

teraction. Two heavy quarks with different flavor can also be in a $J=0$ state, and the corresponding baryons are denoted by us as $\Xi_{bb'}^{'0}$, $\Xi_{bb'}^{'-}$, and $\Omega_{bb'}^{'-}$. The splitting between the spin averaged Ξ_{bb} and the $\Xi_{bb'}'$ (and the corresponding splitting between the Ω's) is due to the heavy-heavy spin interaction. This is expected to be very small, and to vanish in the infinite mass limit.

Our raw data are given in Table XX, and the results for $\Xi_{hh}^* - \Xi_{hh}$, extrapolated to m_l and m_s, are listed in Table XXI. The data show a strong dependence on the heavy quark mass and almost none on the light quark mass. The slope with respect to $1/\bar{M}$ is $0.170(42)\binom{+14}{-21}$ GeV^2 as shown in Fig. 14, and the intercept is $-12(9)\binom{+0}{-1}$ MeV. These results are consistent with those for $\Sigma_h^* - \Sigma_h$. Both are hyperfine splittings between $S=1$ diquark and $S=1/2$ quark sub-systems; the difference is whether the $S=1$ sub-system is heavy-heavy or light-light. In principle the strength of the spin-spin interaction could be different, however, the data suggest that they are similar. In fact this similarity persists even for $h = s$ where $\Xi^* - \Xi = 210$ MeV and $\Sigma^* - \Sigma = 196$ MeV.

If we assume that the spin interaction between the heavy quarks is negligible, then we expect $(\Xi_{hh}^* - \Xi_{hh}) = 1.5(\Xi_{hh'}' - \Xi_{hh})$. The data shown in Table XX indicates a ratio of three instead. Our final estimates are

$$\Xi_{bb} = 10314(46)\binom{-10}{+11} \text{ MeV},$$

$$\Omega_{bb} = 10365(40)\binom{-11}{+12}\binom{+16}{-0} \text{ MeV},$$

TABLE XIX. $\Sigma_h^* - \Sigma_h$ splitting. The preliminary experimental value for $\Sigma_b^* - \Sigma_b$ is 56(8) MeV [3].

	$\Delta E(\Sigma_h^* - \Sigma_h)$									
	Lattice units					MeV				
aM^0	κ_{light}	$\kappa_{av}(m_K)$	$\kappa_{av}(m_{K*})$	$\kappa_s(m_K)$	$\kappa_s(m_{K*})$	κ_{light}	$\kappa_{av}(m_K)$	$\kappa_{av}(m_{K*})$	$\kappa_s(m_K)$	$\kappa_s(m_{K*})$
1.6	0.016(03)	0.015(03)	0.015(03)	0.014(02)	0.014(02)	30(07)	28(05)	28(05)	27(04)	26(04)
2.0	0.012(03)	0.012(03)	0.011(03)	0.011(02)	0.011(02)	23(07)	22(05)	22(05)	21(04)	21(04)
2.7	0.008(03)	0.008(02)	0.008(02)	0.008(02)	0.008(02)	16(06)	15(05)	15(04)	15(04)	15(04)
4.0	0.005(03)	0.005(02)	0.005(02)	0.005(02)	0.005(02)	9(05)	9(04)	10(04)	10(03)	
7.0	0.003(02)	0.004(02)	0.004(02)	0.004(02)	0.004(01)	6(05)	7(04)	7(04)	8(03)	8(03)
10.0	0.002(02)	0.002(02)	0.002(02)	0.002(02)	0.003(01)	3(05)	4(04)	4(04)	5(03)	5(03)

TABLE XX. E_{sim} and splittings for heavy-heavy-light baryons.

aM^0	κ	$aE_{\text{sim}}(\Xi_{hh})$	$a\Delta E(\Xi_{hh}^*\text{-}\Xi_{hh})$	$a\Delta E(\Xi_{hh'}'\text{-}\Xi_{hh})$
1.6	0.13690	0.767(08)	0.015(02)	0.005(01)
2.0		0.788(10)	0.012(02)	0.004(01)
2.7		0.803(10)	0.009(02)	0.003(01)
4.0		0.803(14)	0.007(02)	0.002(01)
7.0		0.767(34)	0.003(02)	0.001(01)
10.0		0.735(86)	0.001(02)	0.000(01)
1.6	0.13750	0.754(10)	0.015(02)	0.006(02)
2.0		0.777(10)	0.012(02)	0.004(02)
2.7		0.788(12)	0.009(02)	0.003(02)
4.0		0.792(15)	0.007(02)	0.002(01)
7.0		0.746(38)	0.003(02)	0.001(01)
10.0		0.717(107)	0.001(02)	0.000(01)
1.6	0.13808	0.747(12)	0.015(02)	0.006(02)
2.0		0.768(14)	0.012(02)	0.004(02)
2.7		0.779(14)	0.009(02)	0.003(02)
4.0		0.774(19)	0.006(02)	0.002(01)
7.0		0.733(47)	0.002(02)	0.001(01)
10.0		0.718(144)	−.001(03)	0.000(01)

$$\Xi_{bb}^* = 10333(55)\binom{-7}{+6}\ \text{MeV},$$

$$\Omega_{bb}^* = 10383(39)\binom{-8}{+8}\binom{+12}{-0}\ \text{MeV},$$

$$\Xi_{bb}^*\text{-}\Xi_{bb} = 20(6)\binom{+2}{-3}\ \text{MeV},$$

$$\Omega_{bb}^*\text{-}\Omega_{bb} = 20(4)\binom{+2}{-3}\ \text{MeV}.$$

VIII. DETERMINATION OF HQET PARAMETERS

We now present a determination of the HQET parameters $\bar{\Lambda}$, λ_1, and λ_2. $\bar{\Lambda}$ denotes the binding energy of the meson in the limit $M^0 = \infty$. In the static theory the $O(1/M)$ corrections to this are given by the expectation value of the heavy quark p^2:

$$-\lambda_1 = \frac{1}{2M_B}\langle B|\bar{b}(i\vec{D})^2 b|B\rangle, \tag{6}$$

and the expectation value of the chromomagnetic operator:

FIG. 12. Spin-averaged $\bar{\Sigma}_h$-Λ_h splitting as a function of the inverse spin-averaged meson mass. The bursts denote experimental values for b and c heavy quarks.

$$\lambda_2 = -\frac{1}{2M_B}\langle B|\bar{b}\vec{\sigma}\cdot\vec{B}b|B\rangle. \tag{7}$$

Thus, to $O(1/M)$, the relation between the heavy quark pole mass m_{pole} and the heavy-light meson mass is given by

$$M_B = \dot{m}_{pole} + \bar{\Lambda} + \frac{1}{2m_{pole}}(-\lambda_1+\lambda_2) \equiv m_{pole} + E_{\text{bind}}. \tag{8}$$

In NRQCD one measures E_{sim}, from which E_{bind} is obtained as

$$E_{\text{bind}} = E_{\text{sim}} - E_0. \tag{9}$$

Using the estimates for E_0 given in Table III, E_{bind} for the spin-averaged H meson is given in Table XXII, and for Λ_h in Table XXIII.

We prefer to analyze the dependence of E_{bind} on the heavy quark mass in terms of $\bar{M}$. The reason for this choice is that m_{pole} is not a physical (measurable) quantity and suffers from a renormalon ambiguity. Also, to $O(1/M)$ the change from m_{pole} to $\bar{M}$ is benign, i.e., the slope still gives the same λ_1 and λ_2 as extracted in conventional HQET analyses. The data for the binding energy for $\bar{H}$, and fits versus $\bar{M}$ are shown in Fig. 15. The behavior of Λ_h is similar. The results for $\bar{\Lambda}$ and λ_1 obtained from these fits are also

TABLE XXI. Ξ_{hh}^*-Ξ_{hh} splitting.

	Ξ_{hh}^*-Ξ_{hh}					
	Lattice units			MeV		
aM^0	κ_{light}	$\kappa_s(m_K)$	$\kappa_s(m_{K*})$	κ_{light}	$\kappa_s(m_K)$	$\kappa_s(m_{K*})$
1.6	0.016(03)	0.015(02)	0.015(02)	31(06)	29(04)	29(04)
2.0	0.012(03)	0.012(02)	0.012(02)	23(05)	23(04)	23(04)
2.7	0.009(03)	0.009(02)	0.009(02)	16(05)	17(04)	17(03)
4.0	0.006(03)	0.007(02)	0.007(02)	11(06)	13(04)	13(04)
7.0	0.001(03)	0.002(02)	0.003(02)	2(06)	5(04)	5(04)
10.0	−.002(05)	0.000(02)	0.001(02)	−4(10)	0(04)	1(04)

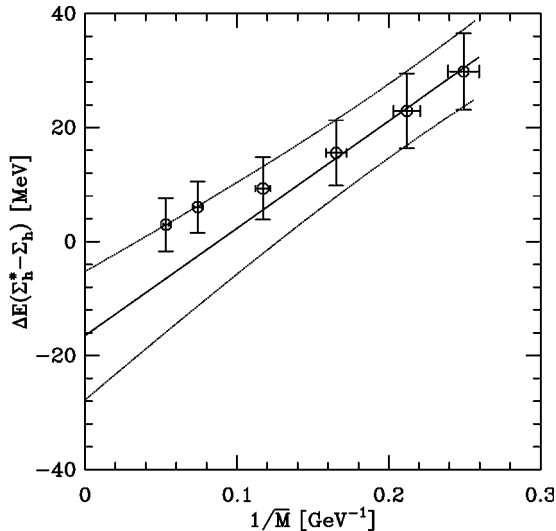TABLE XXII. Binding energies in MeV for the spin-averaged H meson.

aM^0	$E_{bind}(\bar{H})$		
	κ_{light}	$\kappa_s(m_K)$	$\kappa_s(m_{K*})$
1.6	402(19)	496(14)	516(09)
2.0	325(20)	418(11)	439(07)
2.7	378(19)	466(13)	485(09)
4.0	388(21)	476(14)	496(09)
7.0	379(21)	467(13)	487(10)
10.0	375(20)	460(13)	478(09)
$\bar{\Lambda}$	375(25)	458(14)	477(11)
$-\lambda_1$	0.10(33)	0.18(14)	0.20(13)

TABLE XXIII. Binding energies in MeV for the Λ_h baryon.

m_Q^0	$E_{bind}(\Lambda_h)$		
	κ_{light}	$\kappa_{av}(m_K)$	$\kappa_{av}(m_{K*})$
1.6	791(60)	870(47)	907(40)
2.0	692(66)	798(52)	833(45)
2.7	749(80)	852(62)	885(54)
4.0	801(120)	886(94)	915(82)
7.0	817(109)	888(82)	912(73)
10.0	859(149)	908(109)	925(97)
$\bar{\Lambda}$	895(218)	926(148)	937(130)
$-\lambda_1$	$-1.7(3.4)$	$-0.8(2.2)$	$-0.5(1.8)$

given in Tables XXII and XXIII. Note that the slope for spin-averaged cases gives λ_1 since there is no contribution from the chromomagnetic operator.

Our definition of the parameters $\bar{\Lambda}$ and λ_1 is perturbative and they inherit a renormalon ambiguity from E_0 which could be as large as $O(\Lambda_{QCD})$ in $\bar{\Lambda}$. With this definition, estimates of the HQET parameters are

$$\bar{\Lambda}(B) = 375(25)(50)(^{+16}_{-22})\ \text{MeV},$$

$$-\lambda_1(B) = 0.1(3)(1)(^{+1}_{-1})\ \text{GeV}^2,$$

$$\bar{\Lambda}(\Lambda_b) = 895(218)(50)(^{+37}_{-56})\ \text{MeV},$$

$$-\lambda_1(\Lambda_b) = -1.7(34)(1)(^{+2}_{-2})\ \text{GeV}^2. \tag{10}$$

We have quoted, as the second error, a systematic uncertainty due to the unknown $O(\alpha_s^2)$ error in the perturbative expansion of E_0, which we take to be $1 \times \alpha_s^2$. The third error is due to the scale uncertainty. We emphasize that, due to the

renormalon ambiguity, these estimates are only meant to be indicative and cannot be compared directly with other calculations.
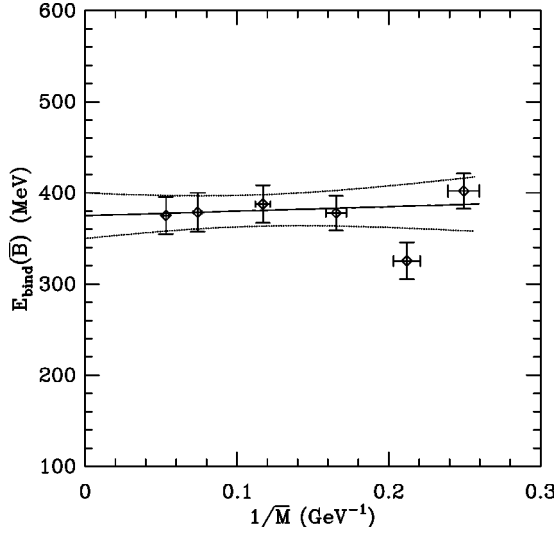
To remove the uncertainty in $\bar{\Lambda}$ and λ_1 due to the perturbative estimate of E_0 we construct differences of binding energies in which E_0 drops out. The intercept of a linear fit to the spin-averaged Λ_h-H and Σ_h-Λ_h splittings versus $1/\bar{M}$ gives

$$\bar{\Lambda}(\Lambda_b)\text{-}\bar{\Lambda}(B) = 415(156)(^{+17}_{-25})\ \text{MeV},$$

$$\bar{\Lambda}(\Sigma_b)\text{-}\bar{\Lambda}(\Lambda_b) = 179(152)(^{+9}_{-10})\ \text{MeV}. \tag{11}$$

In both cases we find no significant dependence on $1/\bar{M}$. This suggests that the corresponding λ_1 are roughly the same. A similar construction for states with different light quarks gives

$$\bar{\Lambda}(B_s)\text{-}\bar{\Lambda}(B_d) = 81(31)(^{-3}_{+5})(^{+18}_{-0})\ \text{MeV},$$

$$\lambda_1(B_s)\text{-}\lambda_1(B_d) = -0.10(28)(^{+2}_{-0})\ \text{GeV}^2. \tag{12}$$

FIG. 13. Σ_h^*-Σ_h splitting as a function of $1/\bar{M}$.

FIG. 14. Ξ_{hh}^*-Ξ_{hh} (circles) and $\Xi_{hh'}'$-Ξ_{hh} (diamonds) splittings as a function of the inverse spin-averaged meson mass along with linear fits.

FIG. 15. E_{bind} versus $1/\bar{M}$.

Lastly, we estimate λ_2 from the slope of the hyperfine splitting calculated in Sec. V D. We find

$$\lambda_2(B_d) = 0.069(19)\binom{+6}{-8} \ \text{GeV}^2,$$

$$\lambda_2(B_s) = 0.078(12)\binom{+6}{-8}\binom{+2}{-0} \ \text{GeV}^2. \tag{13}$$

These parameters have previously been calculated by the Rome Collaboration using HQET [23,43]. They find

$$\bar{\Lambda}(B) = 180\binom{+30}{-20} \ \text{MeV},$$

$$-\lambda_1(B_d) = -0.09(14) \ \text{GeV}^2,$$

$$\lambda_1(B_s)\text{-}\lambda_1(B_d) = -0.09(4) \ \text{GeV}^2,$$

$$\lambda_2(B_d) = 0.070(15) \ \text{GeV}^2. \tag{14}$$

It is important to note that their definition of $\bar{\Lambda}$ and λ_1 includes a non-perturbative subtraction of the ultra-violet divergence. Thus, the only results that can be compared directly are those for $\lambda_1(B_s)\text{-}\lambda_1(B_d)$ and $\lambda_2(B_d)$. The experimental values for these two quantities are

$$\lambda_1(B_s)\text{-}\lambda_1(B_d) = 2\frac{(\bar{M}_{B_s} - \bar{M}_B) - (\bar{M}_{D_s} - \bar{M}_D)}{1/\bar{M}_D - 1/\bar{M}_D}$$

$$= -0.06(2) \ \text{GeV}^2,$$

$$\lambda_2(B_d) = \frac{M_{B^*_d}^2 - M_{B_d}^2}{4} = 0.12(1) \ \text{GeV}^2. \tag{15}$$
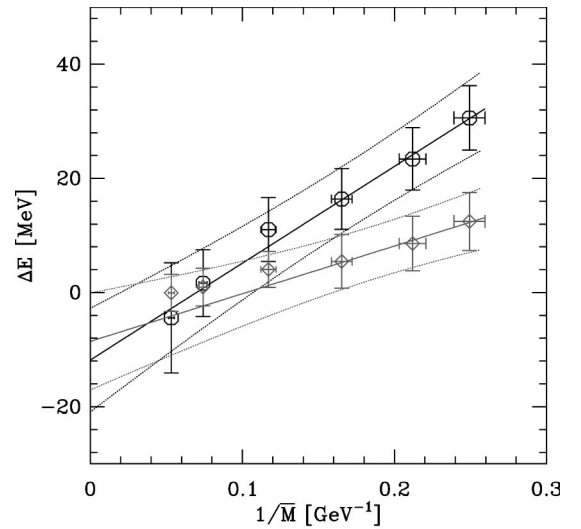
IX. CONCLUSIONS

We have presented an analysis of heavy-light mesons and baryons using a non-relativistic formulation (NRQCD) for the bottom quark. Estimates of meson masses with one b quark and baryons with one or two b quarks are given in Tables IX and XVI. Using the B meson to fix the b quark mass, we estimate $m_{\overline{MS}}(m_{\overline{MS}}) = 4.35(10)\binom{-3}{+2}(20)$ GeV. This is consistent with previous lattice determinations of m_b using the Υ binding energy [19,20,22], or HQET [22,23,24]. A more direct comparison will be possible after we extract, using the same set of lattices and propagators, m_b from the Υ binding energy.

A significant feature of our calculation is that we can resolve the P states. We find that $M_{B^*_0} < M_{B^*_2}$. Using the interpolating operators based on the LS coupling scheme, we could not distinguish between the 1^+ and $1^{+'}$ states, as these mix. Also, we resolve b baryon hyperfine splittings for the first time on the lattice.

The mass splittings are analyzed in terms of a qualitative picture based on a non-relativistic quark model that is described in Sec. V. We find that the dependence of the splittings on the light and heavy quark masses are in agreement with this picture. Quantitatively, the radial $(2S\text{-}1S)$, orbital $(P\text{-}S)$, $\bar{\Sigma}\text{-}\Lambda$, and $\Lambda\text{-}\bar{B}$ splittings are found to be within 1σ ($\sim 20\%$) of the experimental values.

We are able to resolve hyperfine splittings in both mesons and baryons. The most significant difference from experimental numbers is in the $B^*\text{-}B$ hyperfine splitting. Such an underestimate of hyperfine splittings is a general feature of quenched calculations (light-light, heavy-light and heavy-heavy). Another uncertainty associated with the quenched approximation is in fixing the strange quark mass. As a result, splittings which are sensitive to the light quark mass have an uncertainty of up to roughly 20% when extrapolated to the strange quark mass.

We have calculated the HQET parameters $\bar{\lambda}$, λ_1, and λ_2 for both the B and Λ_b. $\bar{\Lambda}$ and λ_1 have large uncertainties due to the perturbative determination of the shift in the energy of the heavy quark, E_0. The differences in these quantities between different hadrons do not have this ambiguity and are, therefore, much better determined.

[1] G. P. Lepage *et al.*, Phys. Rev. D **46**, 4052 (1992).

[2] A. Ali Khan *et al.*, Phys. Lett. B **427**, 132 (1998).

[3] DELPHI Collaboration, DELPHI Note 95–107, contribution to EPS'95, http://home.cern.ch/pubxx/www/delsec/conferences/brussels/pap_t11-9.ps.gz.

[4] A. Falk, proceedings of ''B Physics and CP Violation,'' Honolulu, Hawaii, 1997.

[5] H. J. Schnitzer, Phys. Lett. **76B**, 461 (1978); N. Isgur, Phys. Rev. D **57**, 4041 (1998); D. Ebert, V. O. Galkin, and R. N. Faustov, *ibid.* **57**, 5663 (1998).

[6] C. T. H. Davies *et al.*, Phys. Rev. D **50**, 6963 (1994); **58**, 054505 (1998); A. Spitz *et al.*, Nucl. Phys. B (Proc. Suppl.) **63**, 317 (1998); T. Manke *et al.*, Phys. Lett. B **408**, 308 (1997).

[7] A. Ali Khan, Nucl. Phys. B (Proc. Suppl.) **63**, 71 (1998); T. Draper, *ibid.* **73**, 43 (1999).

[8] C. Michael and J. Peisa, Phys. Rev. D **58**, 034506 (1998).

[9] K. C. Bowler *et al.*, Phys. Rev. D **54**, 3619 (1996).

[10] P. Boyle *et al.*, Nucl. Phys. B (Proc. Suppl.) **63**, 314 (1998).

[11] P. B. Mackenzie *et al.*, Nucl. Phys. B (Proc. Suppl.) **63**, 305 (1998).

[12] H. Wittig, Nucl. Phys. B (Proc. Suppl.) **63**, 47 (1998).

[13] J. Hein *et al.*, hep-ph/0003130 [Phys. Rev. D (to be published)].

[14] K. Hornbostel and G. P. Lepage (in preparation).

[15] C. T. H. Davies *et al.*, Phys. Lett. B **345**, 42 (1995).

[16] G. P. Lepage and P. B. Mackenzie, Phys. Rev. D **48**, 2250 (1993).

[17] M. Beneke and V. M. Braun, Nucl. Phys. **B454**, 253 (1995); M. Beneke, Phys. Rep. **317**, 1 (1999).

[18] N. Gray *et al.*, Z. Phys. C **48**, 673 (1990).

[19] C. T. H. Davies *et al.*, Phys. Rev. Lett. **73**, 2654 (1994).

[20] K. Hornbostel, Nucl. Phys. B (Proc. Suppl.) **73**, 339 (1999).

[21] S. Brodsky *et al.*, Phys. Rev. D **28**, 228 (1983).

[22] Particle Data Group, C. Caso *et al.*, Eur. Phys. J. C **3**, 1 (1998); and 1999 off year partial update for 2000 edition, http://pdg.lbl.gov.

[23] V. Giménez *et al.*, Phys. Lett. B **393**, 124 (1997).

[24] G. Martinelli and C. T. Sachrajda, Nucl. Phys. **B559**, 429 (1999).

[25] A. Ali Khan *et al.* (in preparation).

[26] A. Duncan *et al.*, Nucl. Phys. B (Proc. Suppl.) **30**, 433 (1993).

[27] DELPHI Collaboration, DELPHI 96-93 CONF 22, contribution to ICHEP '96, http://home.cern.ch/pubxx/delsec/conferences/warsaw/pa01-021.ps.gz.

[28] V. Ciulli, Proceedings of the 8th International Symposium on Heavy Flavour Physics, 1999, Southampton, UK, http://www.hep.phys.soton.ac.uk/hf8/talks/talkproc.html.

[29] UKQCD Collaboration, A. K. Ewing *et al.*, Phys. Rev. D **54**, 3526 (1996).

[30] A. Duncan *et al.*, Phys. Rev. D **51**, 5101 (1995).

[31] J. P. Ma and B. H. J. McKellar, Phys. Rev. D **57**, 6723 (1998).

[32] JLQCD Collaboration, K-I. Ishikawa *et al.*, Phys. Rev. D **61**, 074501 (2000).

[33] DELPHI Collaboration, P. Abreu *et al.*, Phys. Lett. B **426**, 231 (1998).

[34] R. Lewis and R. Woloshyn Phys. Rev. D **58**, 074506 (1998).

[35] S. Collins *et al.*, Phys. Rev. D **60**, 074504 (1999).

[36] H. D. Trottier and G. P. Lepage, Nucl. Phys. B (Proc. Suppl.) **63**, 865 (1998).

[37] T. Bhattacharya *et al.*, Phys. Rev. D **53**, 6486 (1996).

[38] J. Rosner, Phys. Lett. B **379**, 267 (1996).

[39] C. Alexandrou *et al.*, Phys. Lett. B **337**, 340 (1994).

[40] E. Jenkins, Phys. Rev. D **55**, 10 (1997).

[41] M. J. Savage and M. B. Wise, Phys. Lett. B **248**, 177 (1990).

[42] A. F. Falk *et al.*, Phys. Rev. D **49**, 555 (1994).

[43] V. Giménez *et al.*, Nucl. Phys. **B486**, 227 (1997).